Comparison of the Therapeutic Response to Treatment with a ^{177}Lu-Labeled Somatostatin Receptor Agonist and Antagonist in Preclinical Models

Simone U. Dalm[1], Julie Nonnekens[1,2], Gabriela N. Doeswijk[1], Erik de Blois[1], Dik C. van Gent[2], Mark W. Konijnenberg[1], and Marion de Jong[1]

[1]*Department of Nuclear Medicine and Radiology, Erasmus MC, Rotterdam, The Netherlands; and* [2]*Department of Genetics, Erasmus MC, Rotterdam, The Netherlands*

Peptide receptor scintigraphy and peptide receptor radionuclide therapy using radiolabeled somatostatin receptor (SSTR) agonists are successfully used in the clinic for imaging and treatment of neuroendocrine tumors. Contrary to the paradigm that internalization and the resulting accumulation of radiotracers in cells is necessary for efficient tumor targeting, recent studies have demonstrated the superiority of radiolabeled SSTR antagonists for imaging purposes, despite little to no internalization in cells. However, studies comparing the therapeutic antitumor effects of radiolabeled SSTR agonists versus antagonists are lacking. The aim of this study was to directly compare the therapeutic effect of ^{177}Lu-DOTA-octreotate, an SSTR agonist, and ^{177}Lu-DOTA-JR11, an SSTR antagonist. **Methods:** We analyzed radiotracer uptake (both membrane-bound and internalized fractions) and the produced DNA double-strand breaks, by determining the number of p53 binding protein 1 foci, after incubating SSTR2-positive cells with ^{177}Lu-diethylene triamine pentaacetic acid, ^{177}Lu-DOTA-octreotate, or ^{177}Lu-DOTA-JR11. Also, biodistribution studies were performed in tumor-xenografted mice to determine the optimal dose for therapy experiments. Afterward, in vivo therapy experiments comparing the effect of ^{177}Lu-DOTA-octreotate and ^{177}Lu-DOTA-JR11 were performed in this same animal model. **Results:** We found a 5-times-higher uptake of ^{177}Lu-DOTA-JR11 than of ^{177}Lu-DOTA-octreotate. The major part (88% ± 1%) of the antagonist uptake was membrane-bound, whereas 74% ± 3% of the total receptor agonist uptake was internalized. Cells treated with ^{177}Lu-DOTA-JR11 showed 2 times more p53-binding protein 1 foci than cells treated with ^{177}Lu-DOTA-octreotate. Biodistribution studies with ^{177}Lu-DOTA-JR11 (0.5 μg/30 MBq) resulted in the highest tumor radiation dose of 1.8 ± 0.7 Gy/MBq, 4.4 times higher than the highest tumor radiation dose found for ^{177}Lu-DOTA-octreotate. In vivo therapy studies with ^{177}Lu-DOTA-octreotate and ^{177}Lu-DOTA-JR11 resulted in a tumor growth delay time of 18 ± 5 and 26 ± 7 d, respectively. Median survival rates were 43.5, 61, and 71 d for the control group, ^{177}Lu-DOTA-octreotate group, and the ^{177}Lu-DOTA-JR11–treated group, respectively. **Conclusion:** On the basis of these results, we concluded that the use of radiolabeled SSTR antagonists such as JR11 might enhance peptide receptor scintigraphy and peptide receptor radionuclide therapy of neuroendocrine tumors and provide successful imaging and therapeutic strategies for cancer types with relatively low SSTR expression.

Received Sep. 16, 2015; revision accepted Oct. 19, 2015.

For correspondence or reprints contact: Simone U. Dalm, Erasmus MC, Rm. Na620, P.O. Box 2040, 3000 CA Rotterdam, The Netherlands.

E-mail: s.dalm@erasmusmc.nl

Published online Oct. 29, 2015.

Key Words: PRRT; somatostatin receptor; agonist; antagonist; therapy

J Nucl Med 2016; 57:260–265
DOI: 10.2967/jnumed.115.167007

Radiolabeled somatostatin (SST) analogs targeting SST receptors (SSTRs), especially SSTR2, overexpressed on tumor cells are successfully used for imaging and treatment of neuroendocrine tumors. These applications are referred to as peptide receptor scintigraphy (PRS) and peptide receptor radionuclide therapy (PRRT), respectively. PRS using radiolabeled SST analogs was first described in the late 1980s by Krenning et al. (*1*), and soon after the first studies using radiolabeled SST analogs for PRRT followed. ^{111}In-diethylene triamine pentaacetic acid (DTPA)-octreotide was the first SSTR radioligand used for therapy and although results were positive, partial remissions were uncommon. Over time multiple SST analogs with improved receptor affinity, mostly receptor agonists, have been developed and described. These SST analogs have been coupled to different chelators, enabling labeling of the SST analogs with positron emitters, such as ^{68}Ga for PET scanning, and β-emitters, such as ^{90}Y and ^{177}Lu for therapeutic purposes, leading to better imaging and therapy results. Concerning therapy, response rates between 10% and 35% have been reported after treatment of gastroenteropancreatic neuroendocrine tumors using ^{90}Y-DOTATOC or ^{177}Lu-DOTA-octreotate (*2,3*). Although results are positive, there is room for improvement of PRRT using SSTR radioligands. Recent developments to improve therapeutic outcome with SSTR radioligands include the use of a combination of ^{90}Y- and ^{177}Lu-labeled peptide analogs, PRRT using α-emitters, and the combination of PRRT with other anticancer agents (*4*). Another recent development is the introduction of SST analogs with receptor antagonistic properties. For decades it was believed that radiolabeled receptor agonists would be superior to antagonists, because they are internalized upon receptor binding, resulting in accumulation of radioactivity in tumor cells. However, recent in vitro and human studies surprisingly showed higher tumor uptake of SSTR antagonists than SSTR agonists (*5–8*). Wild et al. (*8*) reported a 1.7- to 10.6-fold-higher tumor dose when patients were scanned with ^{177}Lu-DOTA-JR11, an SSTR antagonist, than with ^{177}Lu-DOTA-octreotate, an SSTR agonist. Furthermore, in this same study it was demonstrated that therapy with ^{177}Lu-DOTA-JR11 is feasible (*8*).

To date, to our knowledge no study, neither preclinical nor clinical, has been performed comparing therapeutic responses between radiolabeled SSTR agonists and SSTR antagonists. The aim of this study was to compare the therapeutic effect of ^{177}Lu-DOTA-octreotate and ^{177}Lu-DOTA-JR11 in vivo in the H69 SSTR–positive mouse xenograft model. We first determined the optimal peptide amount for therapy using these radiotracers by performing biodistribution studies. Also, in vitro experiments were performed studying the uptake and the DNA damage response after treatment with the radiotracers.

MATERIALS AND METHODS

Radioligands

The SSTR agonist DOTA-octreotate (molecular weight, 1,436 g/mol) (BioSynthema) and the SSTR antagonist JR11 (molecular weight, 1,690 g/mol) (*9*) (kindly provided by Dr. Helmut Maecke) were radiolabeled with ^{177}Lu (IDB), using quenchers to prevent radiolysis, as previously described (*8,10,11*). Specific activity was 53 MBq/nmol for in vitro studies and 0.5 μg/30 MBq, 1.0 μg/30 MBq, and 2.0 μg/30 MBq for in vivo studies. Instant thin-layer chromatography on silica gel and high-pressure liquid chromatography were used to measure radiometal incorporation (>95%) and radiochemical purity (>90%) as previously described (*11*).

Cell Lines and Cell Culture

The SSTR2 complementary DNA sequence from image clone 3875163 (Life Technologies) was cloned into the pcDNA3.1 vector (Life Technologies). Human osteosarcoma cells (U2OS) were transfected with the pcDNA3.1-SSTR2 vector using X-treme GENE HP Transfection Reagent (Roche Life Sciences) and selected for 2 wk with Geneticin (Life Technologies). Single cell colonies were grown to obtain a pure SSTR2-positive cell line (U2OS+SSTR2). Cells were cultured in Dulbecco modified Eagle medium (Lonza), supplemented with 10% fetal bovine serum (Biowest) and 5 mL of penicillin (5,000 units/mL) and streptomycin (5,000 μg/mL) (Sigma Aldrich), at 37°C and 5% CO_2.

Uptake Assay

The membrane-bound and internalized fractions of the radiotracers were determined after incubation of the cells with 4 different concentrations of ^{177}Lu-DOTA-octreotate or ^{177}Lu-DOTA-JR11. To demonstrate SSTR specificity of the uptake, cells were also incubated with equal amounts of ^{177}Lu-DTPA.

Cells were seeded in 12-well plates 1 d before the experiment. The next day, adhered cells (8×10^4 cells/well) were incubated with 5×10^{-8}M/2.5 MBq, 2×10^{-8}M/1 MBq, 5×10^{-9}M/0.25 MBq, or 2×10^{-9}M/0.1 MBq of ^{177}Lu-DOTA-octreotate, ^{177}Lu-DOTA-JR11, or equal amounts of ^{177}Lu-DTPA in 1 mL of culture medium for 4 h at 37°C. After incubation, supernatant was removed and cells were washed twice with phosphate-buffered saline (PBS) (Lonza). Membrane-bound radiotracer fraction was separated from the internalized fraction by incubating cells for 10 min with an acid solution (50 mM glycine and 100 mM NaCl, pH 2.8). Subsequently, cells were lysed using 0.1 M NaOH to collect the internalized radiotracer fraction. Membrane-bound and internalized radiotracer fractions were counted in a γ-counter (1480 WIZARD automatic γ counter; PerkinElmer) using a radionuclide-specific energy window, a counting time of 60 s, and a counting error of 5% or less. Data are expressed as percentage added dose.

DNA Damage Immunofluorescent Staining

DNA double-strand break (DSB) formation was determined by quantifying the number of p53-binding protein 1 (53BP1) foci per nucleus over time in cells treated with the radiotracers. 53BP1 is a key protein that is recruited to DSB during early repair and is therefore a good marker for DSBs (*12*). Its accumulation on the DSB is visualized as nuclear foci.

To measure DNA DSBs, cells were seeded on glass coverslips in 6-well plates 1 d before the experiment. The next day, adhered cells were incubated with 5 MBq of ^{177}Lu-DTPA, 7.9×10^{-8}M/5 MBq of ^{177}Lu-DOTA-octreotate, or 7.9×10^{-8}M/5 MBq of ^{177}Lu-DOTA-JR11 in 2 mL culture medium for 4 h at 37°C. Subsequently, cells were washed twice with PBS and incubated for different time points (0, 1, 2, and 3 d) in culture medium without radiotracers. Cells were fixed with 1 mL of 2% paraformaldehyde (Sigma Aldrich) for 15 min at room temperature (RT), permeabilized in PBS containing 0.1% Triton X-100 (Sigma Aldrich) by incubating twice for 10 min at RT, and incubated in blocking buffer (PBS, 0.1% Triton X-100, 2% bovine serum albumin [Sigma Aldrich]) for 30 min at RT. Next, cells were incubated for 90 min at RT with the primary antibody, anti-53BP1 (NB100-304 [Novus Biologicals]; 1/1,000) diluted in blocking buffer. After incubation, cells were washed 3 times for 5 min at RT with PBS and 0.1% Triton X-100 and incubated with the secondary antibody (goat antirabbit Alexa Fluor 594 [Life Technologies]; 1/1,000) in blocking buffer for 60 min at RT. Cells were mounted with Vectashield (Vector Laboratories) containing DAPI (4′,6-diamidino-2-phenylindole). Z-stack imaging was performed using a TCS SP5 confocal microscope (Leica), and foci were counted from 30 to 40 cells per condition using Image J software (National Institutes of Health). Foci were considered legitimate when their size was between 20 and 100 squared pixels; foci smaller or bigger were considered background staining.

In Vivo Biodistribution Studies

All animal experiments were approved by the Animal Welfare Committee of the Erasmus MC, and all experiments were conducted in accordance to accepted guidelines.

BALB c *nu/nu* male animals, subcutaneously (right shoulder) inoculated with 4×10^6–4×10^7 cells of the SSTR2-positive human small cell lung cancer cell line H69, were used in this study. Tumors were allowed to grow for 3–4 wk after cell inoculation. Tumor size was 241 ± 151 mm^3 for biodistribution studies and 701 ± 387 mm^3 for in vivo therapy studies.

To determine the optimal radiotracer peptide amount for therapy, biodistribution studies were performed. Because studies determining the optimal dose for ^{177}Lu-DOTA-octreotate were previously performed at our department, biodistribution studies were performed only for ^{177}Lu-DOTA-JR11. For this, animals were injected with 0.5 μg/30 MBq, 1 μg/30 MBq, or 2 μg/30 MBq of ^{177}Lu-DOTA-JR11. At 4 time points (4 h, 2 d, 4 d, and 7 d) after injection, animals (n = 4 per peptide amount for each time point) were euthanized, and tumors and organs were collected, weighed, and counted in a γ-counter as previously mentioned. The radioactivity uptake in tumor and organs was determined and expressed as percentage injected dose per gram of tissue (%ID/g).

In Vivo Therapy Studies

In the therapy experiment, 24 BALB c *nu/nu* male mice with subcutaneous H69 xenografts were intravenously injected with 0.5 μg/30 MBq of ^{177}Lu-DOTA-JR11, 0.5 μg/30 MBq of ^{177}Lu-DOTA-octreotate, or 200 μL of injection fluid (sham) (n = 8 each group). Animals injected with either one of the radiotracers were preinjected with 4 mg of modified fluid gelatin (Gelofusin; Braun) to reduce renal uptake (*13*). Tumor size, weight, and physical well-being of the animals were monitored 3 times per week. Mice were euthanized when tumor size reached 2,000 mm^3 or animal weight decreased by 10% or more.

Dosimetry

Absorbed doses were calculated for both compounds in organs with physiologic uptake and in the tumor xenografts. Organ dosimetry was performed according to the MIRD principle following the equation for absorbed dose in organ j as a summation from all source organs i: $D_j = A \sum_i \tilde{a}_i \times S(j \leftarrow i)$.

Time–activity curves were determined by least-squares fitting of single-exponential curves through the data, using Prism software (GraphPad). The time-integrated activity coefficients $\tilde{a}_i$ in each source organ i were determined by integration of the exponential curves folded with the ^{177}Lu decay (half-life, 6.647 d). The S value ^{177}Lu dose factors were taken from the 25-g RADAR stylized mouse phantom (*14*). The absorbed doses in the tumor xenografts were determined using the spheric node option within the Olinda/EXM software (*15*).

Statistics

Tumor growth curves were individually determined by least-squares fitting of single-exponential growth curves to the tumor size measurements against time. The growth curves of animals were extrapolated to later times beyond the censoring endpoint due to the maximum tumor volume of 2,000 mm^3. The extrapolated data were combined with the data of the longest surviving animals to obtain a collective growth curve within each group. Group-averaged mean values of tumor size as a function of time were considered only for normally distributed tumor volumes at each time point using the Shapiro–Wilk normality test. A Pearson correlation coefficient $R^2 > 0.8$ was used for acceptance of the fits. The growth delay time was defined as the difference in time to reach the maximum tumor volume of 2,000 mm^3 between the treatment group and the control. Significant differences were evaluated using the 1-way ANOVA test, after checking for normality by the Shapiro–Wilk normality test. All statistical evaluations were performed with Prism software.

RESULTS

In Vitro Uptake of ^{177}Lu-DOTA-Octreotate and ^{177}Lu-DOTA-JR11

In the in vitro assay, tumor cell uptake of both ^{177}Lu-DOTA-octreotate and ^{177}Lu-DOTA-JR11 was observed. Little to no uptake was seen, on the other hand, when cells were incubated with ^{177}Lu-DTPA, demonstrating receptor specificity of the radiotracers. The total uptake of ^{177}Lu-DOTA-JR11 was up to 5 times higher than the ^{177}Lu-DOTA-octreotate uptake (Fig. 1). Furthermore, the lowest peptide amount added resulted in the highest percentage added dose uptake of both radiotracers. Most radioactivity uptake of ^{177}Lu-DOTA-octreotate, 74% ± 3%, was internalized, whereas most, 88% ± 1%, of ^{177}Lu-DOTA-JR11 uptake was membrane-bound, in line with the receptor agonistic versus receptor antagonistic properties of the 2 radiotracers.

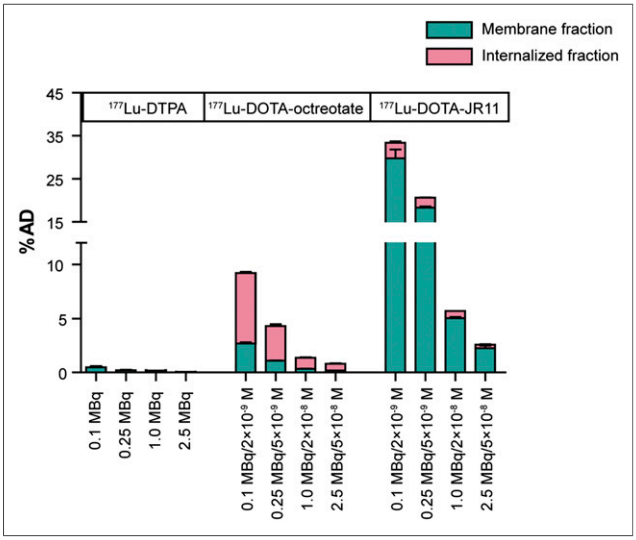

FIGURE 1. Uptake of SSTR agonist ^{177}Lu-DOTA-octreotate and SSTR antagonist ^{177}Lu-DOTA-JR11 in the SSTR2-transfected U2OS cell line. %AD = percentage added dose.

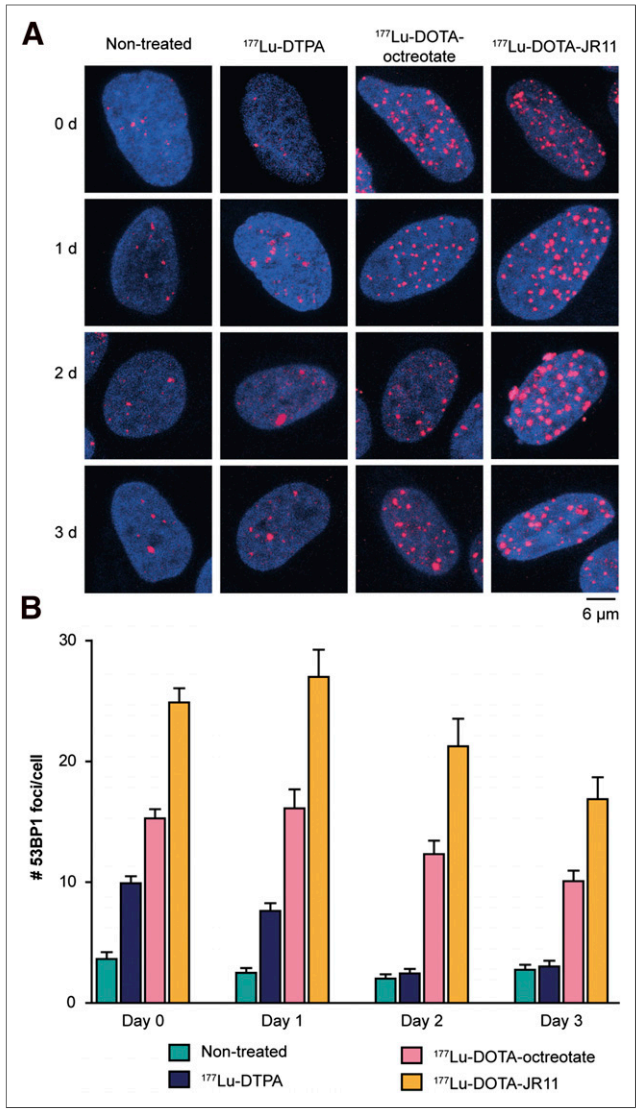

FIGURE 2. DNA damage response studied by analyzing 53BP1 foci in U2OS+SSTR2 cells after treatment with ^{177}Lu-DOTA-octreotate and ^{177}Lu-DOTA-JR11. Nontreated and ^{177}Lu-DTPA–treated cells were taken along as control. (A) Pictures of 53BP1 and DAPI (nuclear) staining of treated and untreated samples at different time points after treatment. 53BP1 is in red, DAPI is in blue. (B) Quantification of 53BP1 foci in 30–40 cells per condition after treatment. Error bars represent SEM.

DNA Damage Response

The timing and level of DNA DSB induction and repair were quantified by counting the number of 53BP1 foci per nucleus over time (Fig. 2). Initially, DSBs were induced by ^{177}Lu-DTPA, ^{177}Lu-DOTA-octreotate, and ^{177}Lu-DOTA-JR11. However, after unbound radioactivity/radiotracers were removed, the ^{177}Lu-DTPA–induced DSBs were repaired within a day, whereas DSBs caused by ^{177}Lu-DOTA-octreotate and ^{177}Lu-DOTA-JR11 remained present for at least 3 d. In line with the difference in uptake, ^{177}Lu-DOTA-JR11 treatment produced more DSBs than ^{177}Lu-DOTA-octreotate treatment, and this increased level of DSBs remained over time.

In Vivo Biodistribution and Dosimetry of ^{177}Lu-DOTA-JR11

Biodistribution studies were performed at 4 different time points after injection of 0.5 μg/30 MBq, 1.0 μg/30 MBq, or 2.0 μg/30 MBq of ^{177}Lu-DOTA-JR11. Injection of 0.5 μg/30 MBq of the radiotracer resulted in the highest tumor uptake, with the lowest variation (20.8 ± 3.4 %ID/g of tissue 4 h after injection). Next to the tumor uptake, high uptake was seen in the kidneys (31.1 ± 5.5 %ID/g of tissue 4 h after injection), as a consequence of urinary excretion and partial reabsorption of the radiotracer, and in the SSTR2-expressing pancreas (9.28 ± 1.22 %ID/g of tissue 4 h after injection) and stomach (7.74 ± 1.00 %ID/g of tissue 4 h after injection). Kidney, stomach, and pancreas radioactivity decreased relatively quickly, with clearance half-lives ranging between 14 and 19 h, whereas tumor uptake remained longer, with a clearance half-life of 30 h. Seven days after injection of 0.5 μg/30 MBq of ^{177}Lu-DOTA-JR11, tumor radioactivity was 6.8 ± 2.5 %ID/g of tissue, whereas kidney, stomach, and pancreas uptake was 1.20 ± 0.26, 0.64 ± 0.20, and 0.32 ± 0.07 %ID/g of tissue, respectively. The results of the biodistribution study are displayed in Table 1. Dosimetry calculations resulted in a tumor radiation dose of 1.8 ± 0.7 Gy/MBq using 0.5 μg of the radiotracer. The tumor and highest organ doses for the different peptide amounts are indicated in Table 2. The tumor, pancreas, and stomach doses were reduced considerably by higher peptide amount, whereas the dose to the kidney remained constant.

In Vivo Therapy Studies

BALB c *nu/nu* animals with H69 xenografts received either a sham injection, a therapeutic injection of 0.5 μg/30 MBq of ^{177}Lu-DOTA-octreotate, or 0.5 μg/30 MBq of ^{177}Lu-DOTA-JR11, the optimal peptide amount previously reported for ^{177}Lu-DOTA-octreotate and the optimal peptide amount measured in biodistribution studies for ^{177}Lu-DOTA-JR11. Animals treated with ^{177}Lu-DOTA-JR11 showed a decrease in tumor size up to 45 ± 7 d after injection after which tumor regrowth occurred (Fig. 3A). For ^{177}Lu-DOTA-octreotate, tumor regrowth was already observed 41 ± 2 d after injection of the radiotracer. Furthermore, median survival rates were 43.5, 61, and 71 d for the control group, the ^{177}Lu-DOTA-octreotate group, and the ^{177}Lu-DOTA-JR11–treated group, respectively (Fig. 3B).

The mean time to reach 2,000 mm^3 was 45 ± 10 d for control animals, 64 ± 14 d for ^{177}Lu-DOTA-octreotate, and 71 ± 10 d for ^{177}Lu-DOTA-JR11–treated animals. Hence, the growth delay times were 18 ± 5 and 26 ± 7 d for ^{177}Lu-DOTA-octreotate and ^{177}Lu-DOTA-JR11–treated groups, respectively. This was significantly different from the control group but did not show a significant difference between the 2 compounds.

DISCUSSION

Previous studies demonstrated SSTR antagonists to be superior to SSTR agonist for tumor targeting, contradicting the paradigm that internalization and accumulation of the radiotracer is necessary for efficient tumor targeting. However, up to now no study has been performed directly comparing the therapeutic effect of radiolabeled SSTR agonists and antagonists. In this study, we compared the therapeutic response of the radiolabeled SSTR agonist ^{177}Lu-DOTA-octreotate and the radiolabeled SSTR antagonist ^{177}Lu-DOTA-JR11 in vitro, in U2OS+SSTR2 cells, and in vivo in H69-xenografted mice.

First, we studied the in vitro uptake of the 2 radiotracers and found uptake to be up to 5 times higher with ^{177}Lu-DOTA-JR11 than with ^{177}Lu-DOTA-octreotate. We saw that the major part of ^{177}Lu-DOTA-octreotate was internalized, whereas the major part of the total uptake of ^{177}Lu-DOTA-JR11 remained membrane-bound, consistent with the receptor agonistic and antagonistic properties of the 2 peptides. These data are in line with previous findings by Fani et al. (*9*) who demonstrated SSTR2-specific antagonism of Ga-NODAGA-JR11 by immunofluorescence imaging in the presence and absence of the SSTR2 agonist Tyr^3-octreotide.

To compare efficacy of the 2 radiolabeled peptides at the molecular level, we also analyzed the DNA damage response after treating cells with ^{177}Lu-DOTA-octreotate or ^{177}Lu-DOTA-JR11. ^{177}Lu emits β-particles that can induce several types of DNA damage, among which DSBs are the most genotoxic. Unrepaired DSBs can trigger cell cycle arrest, cell death, and chromosomal aberrations. DSB induction initiates a cascade of events, including accumulation of the necessary repair proteins (e.g., 53BP1) (*12*). Quantification of 53BP1 foci per nucleus is therefore a powerful tool to examine DSB induction and repair (*16,17*). ^{177}Lu-DTPA produced only transient DSBs comparable to DSBs induced by an external radiation source (*16*). ^{177}Lu-DOTA-JR11 produced 2 times more DSBs than ^{177}Lu-DOTA-octreotate, even though we observed up to 5-times-higher uptake of the radiolabeled antagonist in the uptake assay. This difference might be explained by the different peptide concentrations used in the assays, because radiotracer

TABLE 1
Biodistribution of ^{177}Lu-DOTA-JR11 in H69-Xenografted Mice

	0.5 μg				1.0 μg				2.0 μg			
Organ	4 h	2 d	4 d	7 d	4 h	2 d	4 d	7 d	4 h	2 d	4 d	7 d
Blood	0.23 ± 0.04	0.03 ± 0.01	0.02 ± 0.01	0.01 ± 0.00	0.11 ± 0.02	0.01 ± 0.00	0.01 ± 0.01	0.01 ± 0.00	0.10 ± 0.08	0.04 ± 0.04	0.01 ± 0.00	0.00 ± 0.00
Spleen	0.56 ± 0.15	0.35 ± 0.08	0.29 ± 0.05	0.30 ± 0.07	0.55 ± 0.07	0.29 ± 0.09	0.24 ± 0.05	0.25 ± 0.04	0.43 ± 0.21	0.23 ± 0.03	0.18 ± 0.05	0.17 ± 0.04
Pancreas	9.28 ± 1.22	1.32 ± 0.13	0.56 ± 0.08	0.32 ± 0.07	8.22 ± 1.20	0.99 ± 0.11	0.47 ± 0.12	0.28 ± 0.02	3.07 ± 1.06	0.39 ± 0.05	0.20 ± 0.05	0.10 ± 0.01
Adrenals	1.58 ± 0.92	0.49 ± 0.26	0.30 ± 0.04	0.19 ± 0.06	2.04 ± 2.25	0.33 ± 0.13	0.22 ± 0.07	0.19 ± 0.05	0.47 ± 0.09	0.24 ± 0.06	0.15 ± 0.05	0.14 ± 0.07
Kidney	31.13 ± 5.50	7.40 ± 1.04	2.74 ± 0.51	1.20 ± 0.26	30.06 ± 3.80	7.23 ± 1.79	2.58 ± 0.18	1.07 ± 0.51	32.56 ± 13.20	6.27 ± 0.54	2.26 ± 0.53	0.84 ± 0.22
Liver	1.93 ± 0.03	0.68 ± 0.08	0.47 ± 0.01	0.35 ± 0.07	2.36 ± 0.24	0.59 ± 0.11	0.43 ± 0.03	0.25 ± 0.03	1.39 ± 0.59	0.42 ± 0.03	0.33 ± 0.03	0.19 ± 0.03
Stomach	7.71 ± 1.00	2.03 ± 0.52	1.10 ± 0.10	0.64 ± 0.20	5.38 ± 1.17	1.22 ± 0.17	1.01 ± 0.12	0.52 ± 0.04	2.30 ± 0.93	0.58 ± 0.09	0.32 ± 0.05	0.21 ± 0.04
Duodenum	0.98 ± 0.31	0.34 ± 0.20	0.11 ± 0.03	0.08 ± 0.01	0.96 ± 0.26	0.14 ± 0.04	0.11 ± 0.03	0.07 ± 0.02	0.48 ± 0.19	0.08 ± 0.01	0.06 ± 0.02	0.03 ± 0.01
Muscle	0.22 ± 0.20	0.05 ± 0.02	0.04 ± 0.01	0.03 ± 0.01	0.20 ± 0.10	0.04 ± 0.01	0.06 ± 0.02	0.03 ± 0.01	0.18 ± 0.15	0.03 ± 0.00	0.02 ± 0.01	0.03 ± 0.01
Tumor	20.78 ± 3.37	11.21 ± 2.68	10.21 ± 6.49	6.75 ± 2.46	21.44 ± 9.84	13.57 ± 3.25	8.61 ± 2.51	6.25 ± 1.55	13.64 ± 6.15	7.05 ± 1.62	4.32 ± 1.10	3.38 ± 1.05
Tail	1.22 ± 0.28	0.33 ± 0.08	0.38 ± 0.20	0.30 ± 0.22	1.27 ± 0.15	0.38 ± 0.21	0.19 ± 0.04	0.17 ± 0.11	1.07 ± 0.28	0.28 ± 0.12	0.10 ± 0.02	0.09 ± 0.06

TABLE 2
Absorbed Dose Per Administered Activity (Gy/MBq) in 220 mg H69 Tumor Xenograft and Organs for ^{177}Lu-DOTA-JR11

Organs	0.5 μg	1.0 μg	2.0 μg
Tumor	1,800	1,645	936
Kidneys	969	925	886
Stomach	249	189	78
Pancreas	238	202	82

uptake is dependent on the peptide amount used (2×10^{-9}M of the radiotracers resulted in a 5-times-higher uptake of ^{177}Lu-DOTA-JR11 vs. ^{177}Lu-DOTA-octreotate, whereas the uptake was only 3 times higher with 5×10^{-8}M of the radiotracers). Furthermore, being a receptor antagonist, ^{177}Lu-DOTA-JR11 remained bound to the cell membrane, whereas the receptor agonist ^{177}Lu-DOTA-octreotate is internalized. The ^{177}Lu coupled to JR11, therefore, resides on average at a larger distance from the nucleus and its DNA content. This might reduce the number of β-particles effectively reaching the DNA to induce damage, especially when cells are grown in 2-dimensional cell culture.

^{177}Lu-DOTA-JR11 biodistribution studies in mice with H69 xenografts resulted in the highest tumor uptake with the lowest variation using 0.5 μg/30 MBq of the radiotracer. This was similar to the 22.4 ± 7.6 ID/g of tissue 2 h after injection of 100 pmol ^{68}Ga-DOTA-JR11 reported by Fani et al. (*9*). Previous biodistribution studies with ^{177}Lu-DOTA-octreotate in the same animal model resulted in the highest tumor uptake of 4.03 ± 0.83 %ID/g of tissue using 0.5 μg/30 MBq of ^{177}Lu-DOTA-octreotate 2 d after injection of the radiotracer (S. Bison, M. Konijnenberg, and M. de Jong, unpublished data, December 2013). At this time point, 0.5 μg/30 MBq of ^{177}Lu-DOTA-JR11 resulted in an almost 3-times-higher tumor uptake of 11.21 ± 2.68 ID/g of tissue in our biodistribution studies. This was higher than the 1.2-times-higher uptake of ^{68}Ga-DOTA-JR11 compared with ^{68}Ga-DOTA-octreotate 2 h after injection of the radiotracers reported by Fani et al. (*9*).

The higher tumor uptake after ^{177}Lu-DOTA-JR11 resulted in a tumor radiation dose of 1.8 ± 0.7 Gy/MBq, 4.4-fold higher than the maximum tumor radiation dose for ^{177}Lu-DOTA-octreotate (0.36 ± 0.07 Gy/MBq). Wild et al. (*8*) reported a 1.7- to 10.6-fold-higher tumor dose of ^{177}Lu-DOTA-JR11 in patients, due to higher tumor uptake and longer residence time of the receptor antagonist, indicating the applicability and translational value of our mouse model.

Next to the tumor, high kidney uptake of ^{177}Lu-DOTA-JR11 was found. To reduce the renal uptake in the in vivo therapy studies, animals were preinjected with modified fluid gelatin. Previous studies showed a decrease in renal uptake of 60% when animals received a preinjection of modified fluid gelatin (*13*). Despite the high renal uptake, the treated animals showed no signs of kidney insufficiency. However, in our study animals received only 1 therapeutic injection of ^{177}Lu-DOTA-JR11, and follow-up time was limited. To accurately determine the effect of the radiotracer on the kidneys, additional experiments are needed. In the pilot study by Wild et al. (*8*), patients were preinjected with a solution of arginine and lysine to reduce renal uptake, resulting in a 6.2-fold-higher tumor-to-kidney ratio for ^{177}Lu-DOTA-JR11 than ^{177}Lu-DOTA-octreotate. Although the patients in this study already had grade 2 or 3 chronic renal failure, no additional decrease in tubular kidney function was reported. Additional studies in larger patient groups without renal problems and studies with longer follow up times are necessary to further investigate potential adverse effects.

Comparing the in vivo therapeutic effect of ^{177}Lu-DOTA-octreotate and ^{177}Lu-DOTA-JR11, we found a longer tumor growth delay time and a longer median survival after ^{177}Lu-DOTA-JR11 treatment. This finding is in line with the higher uptake we found in the in vitro internalization assay and the in vivo biodistribution study. However, the difference in growth delay time between the ^{177}Lu-DOTA-JR11 and ^{177}Lu-DOTA-octreotate–treated animals was not significant. This can be explained by variation in initial tumor size and the fact that animals received only 1 therapeutic injection of the radiotracers. Furthermore, the absorbed dose factor for ^{177}Lu in the cytoplasm (as a consequence of agonist internalization) is 1.5–2 times higher than the absorbed dose factor for ^{177}Lu uptake that is limited to the cell membrane (most of the antagonist uptake) (*18*).

The superiority of receptor antagonists to receptor agonist has also been reported for other radioligands. So, studies evaluating the use of radiolabeled gastrin-releasing peptide receptor agonists and antagonists for targeting of gastrin-releasing peptide receptors overexpressed on prostate cancer cells also showed superiority for antagonists (*19*).

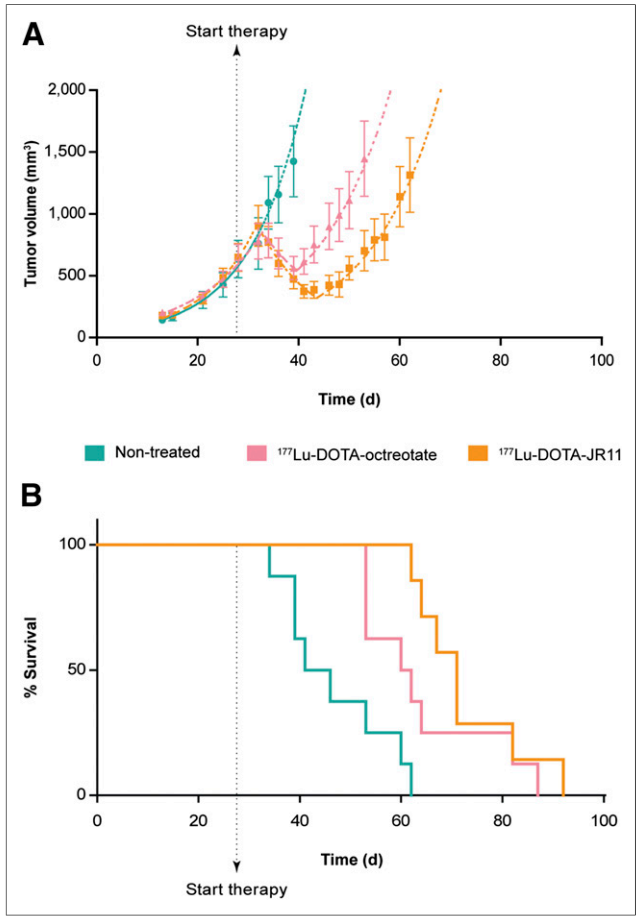

FIGURE 3. (A) Tumor growth extrapolation of control, ^{177}Lu-DOTA-octreotate, and ^{177}Lu-DOTA-JR11–treated animals. ^{177}Lu-DOTA-octreotate and ^{177}Lu-DOTA-JR11–treated animals were preinjected with modified fluid gelatin to reduce renal uptake of radiotracers. (B) Kaplan–Meier survival curve of control animals, ^{177}Lu-DOTA-octreotate, and ^{177}Lu-DOTA-JR11–treated animals.

Studies with unlabeled SSTR antagonists BIM-23454 and BIM-23627 in rats showed an increase in growth hormone secretion after administration (*20*), which may have a negative effect on tumor therapy. However, the minimal effective concentration, 1 mg/kg for BIM-23454 and 0.02 mg/kg for BIM-23627, necessary to promote growth hormone release was much higher than the dose used for imaging and therapy with radiolabeled SSTR antagonists, for example, 150 ± 20 μg for imaging and 2–3 cycles of 105 ± 35 μg for therapy in the study by Wild et al. (*8*).

The higher uptake of radiolabeled SSTR antagonists might offer possibilities for SSTR-mediated PRS and PRRT to be applied in cancer types with lower SSTR expression, for example, breast cancer. Previous studies by Reubi et al. (*21*) reported high-density SSTR expression in 21% of the breast tumors analyzed, whereas in total 75% of the tumors expressed the SSTR. Cescato et al. (*6*) compared binding of the SSTR antagonist ^{177}Lu-DOTA-BASS with the SSTR agonist ^{177}Lu-DOTA-octreotate and reported 11 ± 4-fold-higher binding of the antagonist in 7 breast carcinomas analyzed by in vitro autoradiography. Furthermore, imaging studies in breast cancer patients using SSTR agonists have been performed with varying results (*22,23*). The use of JR11 may improve these results and provide imaging and therapy options for different tumors.

CONCLUSION

The use of radiolabeled SSTR antagonist such as JR11 may contribute to the improvement of PRS and PRRT in neuroendocrine tumors as well as provide opportunities for SSTR-mediated PRS and PRRT in tumor types with relatively low SSTR expression.

DISCLOSURE

The costs of publication of this article were defrayed in part by the payment of page charges. Therefore, and solely to indicate this fact, this article is hereby marked "advertisement" in accordance with 18 USC section 1734. This study was supported by the Netherlands Organization for Scientific Research (ZON-MW grant 40-42600-98-018) and the Erasmus MC grant "The application of radiolabeled peptides in Breast Cancer." Marion de Jong is shareholder in Advanced Accelerator Applications. No other potential conflict of interest relevant to this article was reported.

ACKNOWLEDGMENTS

We thank Melissa van Kranenburg and Stuart Koelewijn for their technical assistance with the in vitro and in vivo assays and Professor Helmut R. Maecke for providing us with the JR11 peptide.

REFERENCES

1. Krenning EP, Bakker WH, Breeman WA, et al. Localisation of endocrine-related tumours with radioiodinated analogue of somatostatin. *Lancet.* 1989;1: 242–244.
2. Kwekkeboom DJ, Mueller-Brand J, Paganelli G, et al. Overview of results of peptide receptor radionuclide therapy with 3 radiolabeled somatostatin analogs. *J Nucl Med.* 2005;46(suppl 1):62S–66S.
3. Bergsma H, van Vliet EI, Teunissen JJ, et al. Peptide receptor radionuclide therapy (PRRT) for GEP-NETs. *Best Pract Res Clin Gastroenterol.* 2012;26: 867–881.
4. Bison SM, Konijnenberg M, Melis M, et al. Peptide receptor radionuclide therapy using radiolabeled somatostatin analogs: focus on future developments. *Clin Transl Imaging.* 2014;2:55–66.
5. Ginj M, Zhang H, Waser B, et al. Radiolabeled somatostatin receptor antagonists are preferable to agonists for in vivo peptide receptor targeting of tumors. *Proc Natl Acad Sci USA.* 2006;103:16436–16441.
6. Cescato R, Waser B, Fani M, Reubi JC. Evaluation of ^{177}Lu-DOTA-sst2 antagonist versus ^{177}Lu-DOTA-sst2 agonist binding in human cancers in vitro. *J Nucl Med.* 2011;52:1886–1890.
7. Wild D, Fani M, Behe M, et al. First clinical evidence that imaging with somatostatin receptor antagonists is feasible. *J Nucl Med.* 2011;52:1412–1417.
8. Wild D, Fani M, Fischer R, et al. Comparison of somatostatin receptor agonist and antagonist for peptide receptor radionuclide therapy: a pilot study. *J Nucl Med.* 2014;55:1248–1252.
9. Fani M, Braun F, Waser B, et al. Unexpected sensitivity of sst2 antagonists to N-terminal radiometal modifications. *J Nucl Med.* 2012;53:1481–1489.
10. de Blois E, Chan HS, de Zanger R, Konijnenberg M, Breeman WA. Application of single-vial ready-for-use formulation of ^{111}In- or ^{177}Lu-labelled somatostatin analogs. *Appl Radiat Isot.* 2014;85:28–33.
11. de Blois E, Chan H, Konijnenberg M, de Zanger R, Breeman W. Effectiveness of quenchers to reduce radiolysis of ^{111}In- or ^{177}Lu-labelled methionine-containing regulatory peptides: maintaining radiochemical purity as measured by HPLC. *Curr Top Med Chem.* 2012;12:2677–2685.
12. Wyman C, Kanaar R. DNA double-strand break repair: all's well that ends well. *Annu Rev Genet.* 2006;40:363–383.
13. van Eerd JE, Vegt E, Wetzels JF, et al. Gelatin-based plasma expander effectively reduces renal uptake of ^{111}In-octreotide in mice and rats. *J Nucl Med.* 2006;47: 528–533.
14. Keenan MA, Stabin MG, Segars WP, Fernald MJ. RADAR realistic animal model series for dose assessment. *J Nucl Med.* 2010;51:471–476.
15. Stabin MG, Konijnenberg MW. Re-evaluation of absorbed fractions for photons and electrons in spheres of various sizes. *J Nucl Med.* 2000;41:149–160.
16. Löbrich M, Shibata A, Beucher A, et al. gammaH2AX foci analysis for monitoring DNA double-strand break repair: strengths, limitations and optimization. *Cell Cycle.* 2010;9:662–669.
17. Barnard S, Bouffler S, Rothkamm K. The shape of the radiation dose response for DNA double-strand break induction and repair. *Genome Integr.* 2013; 4:1–8.
18. Vaziri B, Wu H, Dhawan AP, Du P, Howell RW, Committee SM. MIRD pamphlet No. 25: MIRDcell V2.0 software tool for dosimetric analysis of biologic response of multicellular populations. *J Nucl Med.* 2014;55:1557–1564.
19. Schroeder RP, Müller C, Reneman S, et al. A standardised study to compare prostate cancer targeting efficacy of five radiolabelled bombesin analogues. *Eur J Nucl Med Mol Imaging.* 2010;37:1386–1396.
20. Tulipano G, Soldi D, Bagnasco M, et al. Characterization of new selective somatostatin receptor subtype-2 (sst2) antagonists, BIM-23627 and BIM-23454. Effects of BIM-23627 on GH release in anesthetized male rats after short-term high-dose dexamethasone treatment. *Endocrinology.* 2002;143:1218–1224.
21. Reubi C, Gugger M, Waser B. Co-expressed peptide receptors in breast cancer as a molecular basis for in vivo multireceptor tumour targeting. *Eur J Nucl Med Mol Imaging.* 2002;29:855–862.
22. Skånberg J, Ahlman H, Benjegård S, et al. Indium-111-octreotide scintigraphy, intraoperative gamma-detector localisation and somatostatin receptor expression in primary human breast cancer. *Breast Cancer Res Treat.* 2002; 74:101–111.
23. Van Den Bossche B, van Belle S, de Winter F, Signore A, van de Wiele C. Early prediction of endocrine therapy effect in advanced breast cancer patients using ^{99m}Tc-depreotide scintigraphy. *J Nucl Med.* 2006;47:6–13.